Radiolytic Synthesis of Bimetallic Ag−Pt Nanoparticles with a High Aspect Ratio

C. M. Doudna,[†] M. F. Bertino,*[,†] Frank D. Blum,[‡] A. T. Tokuhiro,[§] Debdutta Lahiri-Dey,[||] Soma Chattopadhyay,[⊥] and Jeff Terry[||,⊥]

Departments of Physics, Chemistry, and Nuclear Engineering, University of Missouri—Rolla, Rolla, Missouri 65409, Physics Department, University of Notre Dame, Notre Dame, Indiana 46556, and Biological, Chemical, and Physical Sciences, Illinois Institute of Technology, Chicago, Illinois 60616

Received: October 25, 2002; In Final Form: January 16, 2003

Aqueous solutions of Ag−Pt ions and poly(vinyl alcohol) were irradiated with gamma rays at dose rates below 0.5 kGy/h to generate nanoparticles. The nanoparticles were characterized with several experimental techniques. Transmission electron microscopy showed that, surprisingly, the nanoparticles were not spherical but had a high aspect ratio. Wirelike structures were generated with lengths up to 3.5 μm and diameters between 3 and 20 nm. Selected-area diffraction showed that the wires were polycrystalline and that individual grains making up the wires had a face-centered cubic (fcc) structure. The optical absorption of samples, with a Ag/Pt mole ratio higher than 80%, exhibited a Ag surface plasmon absorption band centered around 400 nm. The plasmon band broadened with increasing Pt molar ratio and was replaced by a monotonically decaying background for a Pt molar ratio higher than about 30%. Alloying in the Ag−Pt nanoparticles was investigated with X-ray absorption spectroscopy. The Pt L_3 edge (11.564 keV) was excited to determine the local structure around the Pt atoms. A contraction in the first shell of 0.05 Å was observed, which ruled out the formation of a Ag−Pt homogeneous alloy and suggested the formation of core−shell particles. To understand the mechanism of formation of the nanoparticles, several experimental parameters such as the total radiation dose, type of polymer, metal and polymer concentrations, and type of counterions in solution were varied. The most relevant parameters inducing filament growth were the counterions added to the solution, the mole ratio between the two metals, and the capping polymer. For example, spherical particles resulted if $AgNO_3$ was used instead of Ag_2SO_4, if the Ag/Pt mole ratio was higher than 80% or lower than 20%, and if the degree of hydrolysis of the poly(vinyl alcohol) was higher than 98%.

1. Introduction

Metallic nanostructures with high aspect ratios are promising candidates for the development of sensors[1], nanoscopic electrical connections, and catalysts.[2] Several techniques have been developed to synthesize nanoparticles with predefined aspect ratios and crystalline habits. Limiting our discussion to wet chemistry and photolysis synthesis techniques, high aspect ratio nanoparticles are usually produced in a micellar environment,[3−6] sometimes with the aid of preformed seeds.[7−10] There are also reports of nanowires produced with a polyol technique in the presence of metal cluster seeds[11] and by the photoreduction of noble-metal ions in aqueous solution.[12] The above-mentioned synthesis techniques share common features. In general, a noble metal is reduced at a slow rate in the presence of preformed metal clusters, which act as nucleation seeds, and a capping polymer. The aspect ratio of the nanoparticles is, in general, controlled by varying ion and polymer concentrations, the type of polymer, and the velocity of reduction.

In this work, we show that nanoparticles with high aspect ratios can also be produced with the radiolysis method.[3,13−17] Our technique can produce bimetallic nanowires where at least one of the metals is a transition metal. These features are not common among wet chemistry techniques, which are often limited to syntheses of noble, monometallic nanowires. A large number of experiments were carried out to determine the parameters affecting nanowire formation. Parameters included the total gamma ray dose, type of counterions added to the solution, total and relative metal concentrations, and polymer type and concentration. The most relevant parameters were the counterions, the Ag/Pt mole ratio, and the capping polymer. Our experiments show that Ag clusters were formed in the initial stages of reduction and that Pt−Ag, or pure Pt, clusters nucleated or coalesced around the seeds. Nanowire synthesis was also extremely sensitive to the counterions of the solution and to the degree of hydrolysis of the PVA capping polymer. The important role played by the counterions and the polymer suggested that polymer−metal ion complexes and possibly micelles were formed.

2. Experimental Section

Sample Preparation. Aqueous solutions were prepared with $AgNO_3$, Ag_2SO_4, H_2PtCl_6, K_2PtCl_4, and 2-propanol, all purchased from Alfa Aesar. Solutions had a typical total metal ion concentration between 0.5 and 2×10^{-3} mol/L. Samples were prepared with Ag/Pt mole ratios varying from 100 to 0% Ag in steps of 10%. To scavenge $H^\bullet$ and $OH^\bullet$ radicals generated during irradiation, 0.2 mol/L of 2-propanol was added to the solutions. As a capping polymer, seven different types of PVA were tested. Their characteristics are reported in Table 1. Polymer concentra-

* Corresponding author. E-mail: massimo@umr.edu.
[†] Department of Physics, University of Missouri—Rolla.
[‡] Department of Chemistry, University of Missouri—Rolla.
[§] Department of Nuclear Engineering, University of Missouri—Rolla.
[||] University of Notre Dame.
[⊥] Illinois Institute of Technology.

10.1021/jp0273124 CCC: $25.00
Published on Web 03/11/2003

TABLE 1: Types of Poly(vinyl alcohol) Polymers Employed in the Experiments

poly(vinyl alcohol) (brand name)	hydrolysis (%)	molecular weight (amu)[a]	supplier
Celvol 540	87−89	146 000−186 000*	Celanese
	87−89	88 000−97 000	Alfa Aesar
Celvol 205	87−89	31 000−52 000*	Celanese
Celvol 502	87−89	13 000−23 000*	Celanese
Celvol HA-70	99.3+	186 000+*	Celanese
Celvol 165	99.3+	146 000−186 000*	Celanese
	98−99	88 000−97 000	Alfa Aesar

[a] Molecular weights indicated with * are estimated from a viscosity−molecular weight conversion table that can be found at www.celanesechemicals.com.

tions were varied between 2 and 12 g/L, corresponding to a concentration of monomer units between 0.09 and 0.5 mol/L. Because of their photosensitivity, the samples were stored in the dark after mixing. Before and after irradiation, the solutions were free of precipitates. No scattered light was observed in the UV−visible spectra of the samples prior to irradiation. This ruled out the formation of AgCl, which could have resulted from adding a chlorine-containing compound, like H_2PtCl_6, to aqueous solutions containing Ag^+.[14]

Radiolysis. Radiolysis of aqueous solutions is an efficient method to reduce metal ions and form homo- and heteronuclear clusters of transition metals.[3,13−16] In the radiolysis method, aqueous solutions are exposed to γ rays, as shown in eq 1, to create solvated electrons, e_{aq}^-.[14] These solvated electrons, in turn, reduce the metal ions, as shown in eqs 2 and 3. The metal atoms eventually coalesce to form aggregates, as shown in eq 4.

$$H_2O \xrightarrow{\gamma \text{ radiation}} e_{aq}^-, H_3O^+, H^\bullet, OH^\bullet, H_2O_2 \quad (1)$$

$$e_{aq}^- + M^{m+} \rightarrow M^{(m-1)+} \quad (2)$$

$$e_{aq}^- + M^+ \rightarrow M_0 \quad (3)$$

$$nM_0 \rightarrow M_2 \rightarrow \ldots M_n \quad (4)$$

Samples were irradiated with gamma radiation from the fission products of the University of Missouri−Rolla's pool nuclear reactor. The irradiation procedure was as follows: The reactor was operated at 180 kW for about 1 h, and the samples were placed in front of the core 1 h after reactor shutdown to prevent neutron bombardment and activation of the samples. Gamma rays were generated by the decay of the fission products. Most of these products were short-lived, and the gamma ray flux decreased with time. In the experiments described here, the dose rate decreased exponentially from a value of about 0.5 kGy/h in the first hour after shutdown to about 0.05 kGy/h 48 h after shutdown. Exposure to a total dose between 3 and 3.5 kGy typically required 36 to 48 h. Total doses were measured with thermoluminescent dosimeters (TLD) placed in vials adjacent to the samples to be irradiated.

Characterization. Samples were characterized with transmission electron microscopy (TEM), X-ray absorption fine structure (XAFS), and optical absorption spectroscopy. TEM measurements were carried out with a Philips EM430T microscope operated at 300 keV. Samples for TEM measurements were prepared by evaporating under a nitrogen atmosphere one or two drops of solution on a carbon-coated copper grid. Selected-area electron diffraction (SAED) was employed for structural characterization, whereas the chemical composition of the nanoparticles was determined with energy-dispersive X-ray chemical analysis (EDS). SAED and EDS had a spatial resolution of 150 nm. Optical absorption in the visible and near-infrared was measured with a Cary5 spectrophotometer. X-ray absorption fine structure (XAFS) was performed at the MR-CAT undulator beamline at the advanced photon source, Argonne National Laboratory. The undulator parameters were optimized to obtain a large photon flux with nearly constant intensity within the XAFS energy range. A double crystal Si(111) monochromator was utilized for energy selectivity, and a Rh harmonic rejection mirror was used to eliminate the higher harmonics of the desired energy range (Pt L_3 edge). The aqueous samples were sealed in cylindrical plastic bottles before being placed in the X-ray beam. XAFS measurements were performed in fluorescence mode using a 13-element Ge detector. The incident photon intensity was measured by an ion chamber filled with a 80% He/20% N_2 gas mixture.

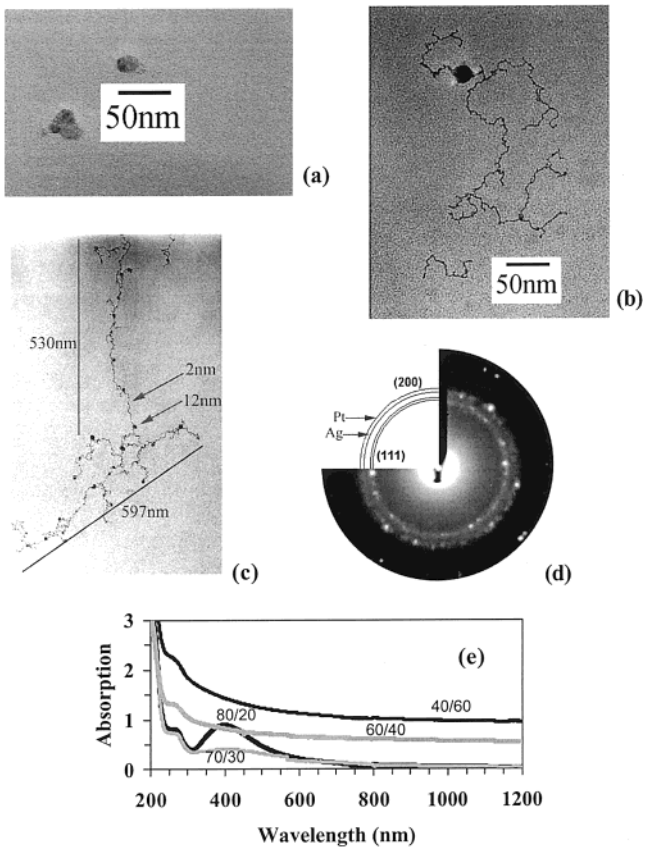

Figure 1. (a) Bright-field TEM micrograph of nanoparticles obtained after exposure to a total dose of 0.5 kGy. (b, c) Bright-field TEM micrographs of nanoparticles obtained after exposure to a dose of 3.5 kGy. (d) Typical SAED of a filament region. (e) Optical absorption of samples with the indicated mole ratios. All solutions contained 0.2 mol/L of 2-propanol, 8 g/L of PVA (MW 88 000−96 000, 87−89% hydrolyzed), and had a total metal ion concentration of 2×10^{-3} mol/L. The mole ratios were $Ag_{0.7}Pt_{0.3}$ (a), $Ag_{0.6}Pt_{0.4}$ (b−d), and $Ag_{0.5}Pt_{0.5}$ (c).

3. Results and Discussion

Figure 1 shows typical bright-field TEM micrographs obtained for different Ag/Pt mole ratios and irradiation times. Figure 1a shows typical nanoparticles produced by irradiating with 0.5 kGy a solution with a total metal concentration of 2×10^{-3} mol/L and a mole ratio of 70% Ag/30% Pt. Nearly spherical particles, with diameters in the 20−30 nm range, were observed. EDS showed that these particles were composed of pure Ag, and SAED yielded diffraction rings characteristic of

a fcc structure. The faster reduction of Ag^+ can be explained on the basis of electrochemical arguments and past experience with the radiolysis method. The reduction of $Pt^{IV}Cl_6^{2-}$ to Pt metal occurs in two steps, which are reported in eqs 5 and 6 together with their standard reduction potentials:

$$Pt^{IV}Cl_6^{2-}/Pt^{II}Cl_4^{2-} \qquad (E^0 = +0.68\ V) \qquad (5)$$

$$Pt^{II}Cl_4^{2-}/Pt^0 \qquad (E^0 = +0.74\ V) \qquad (6)$$

The reduction potential of Ag^+ to Ag metal in acidic solution is $E° = +0.79$ V and is more positive than both Pt reduction steps. Thus, Ag^+ is the more noble species in our solutions. When ionizing radiation at low dose rates is employed to reduce metal ions in aqueous solutions, clusters of the more noble metal (Ag in our case) form first because charge is transferred from the less noble to the more noble species.[14,16] Figure 1b and c shows typical nanoparticles obtained after exposure to a total dose of 3.5 kGy for solutions with the same total metal ion concentration of Figure 1a and various mole ratios. Surprisingly, the nanoparticles are not spherical, but wirelike. The nanowires are composed of two types of particles; large particles, with typical diameters of 20−30 nm, are joined by thin filaments, with diameters of 2−5 nm.

The chemical composition of the nanoparticles was determined with EDS. The spatial resolution of our instrument (about 150 nm) prevented a precise determination of the composition of the larger particles and of the thin filaments. We did establish, however, that regions surrounding large particles have a typical composition of 80−90% Ag, whereas filaments had a typical composition close to 50% Ag. The EDS thus suggested that the larger particles were the Ag particles that formed in the early stages of reduction, and that Pt-rich filaments nucleated out of these Ag particles. Figure 1d shows SAED obtained from a filament region. Diffraction spots are distributed on rings and show that the filaments are polycrystalline. The rings are consistent with fcc structures and indicate that the filaments are made of fcc grains. The low particle density of the filaments and their small diameter resulted in a small number of broad diffraction spots and prevented an accurate determination of lattice parameters with SAED. For example, in the upper left quadrant of Figure 1d, the rings expected for the (111) and (200) reflections of bulk Ag and Pt, respectively, are drawn. Some diffraction spots are broader than the distance between the Ag and Pt rings. It is not possible to determine if the spots originate from reflections of isolated Pt and Ag particles, or from a Ag−Pt alloy with lattice parameter intermediate between those of Ag and Pt. SAED taken from regions surrounding the larger particles yielded results comparable to those obtained for the filaments. Optical absorption of a series of samples with varying Ag/Pt mole ratios is shown in Figure 1e. The absorption spectra of samples rich in Ag show a surface plasmon around 400 nm. This plasmon band broadens with increasing Pt mole fraction and is eventually replaced by a monotonic decay for Pt mole fractions higher than about 30%. Overall,[18] the optical absorption is in excellent agreement with the results of ref 14 and rules out the presence of isolated Ag clusters, which would otherwise give rise to a Ag surface plasmon peak for a very wide range of mole fractions. For example, the Ag surface plasmon is detected for mole fractions as low as 10% Ag when solutions containing pure Ag and pure Pt clusters were mixed.[19] Although helpful, optical absorption measurements could not establish whether Ag and Pt form a homogeneous alloy or if the nanoparticles have a core−shell structure. The surface plasmon

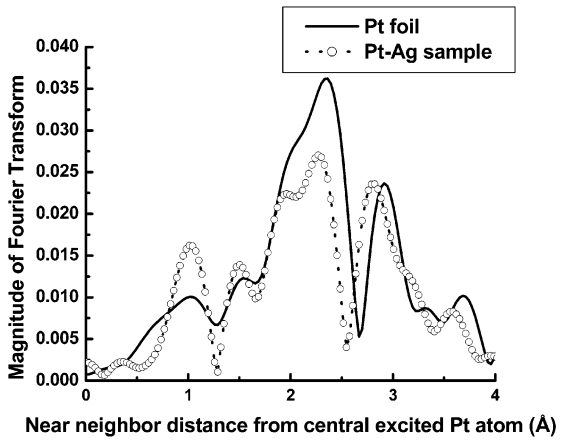

Figure 2. Fourier transform of Pt foil data (—) and of a $Ag_{0.6}Pt_{0.4}$ Pt−Ag sample (- -○- -) over the k range of 3−11.8 $Å^{-1}$.

of Ag nanoparticles is, in fact, extremely sensitive to the presence of transition metals and vanishes rapidly when Pt is added to Ag nanoparticles, independent of cluster structure and degree of alloying.[16,20]

To determine whether the grains making up the filaments were Ag−Pt homogeneous alloys, XAFS of a $Ag_{0.6}Pt_{0.4}$ sample was measured. XAFS is an oscillatory structure in the X-ray absorption spectrum above the absorption edge of the constituent atoms in a material and is defined as the fractional deviation in the absorption coefficient of an atom in a material from its atomic absorption. It is given by $\chi(k) = (\mu - \mu_0)/\mu_0$ (k: photoelectron wavenumber; μ_0: atomic absorption coefficient).[21] The deviation from the atomic absorption results from the fact that when the excited atom is not isolated the photoelectron wave is backscattered by the surrounding atoms. The backscattered wave interferes with the outgoing photoelectron wave and thus gives rise to oscillations in the final state of the system. The period of these oscillations is a function of the bond lengths of the neighbors of the absorbing atom, and the amplitude depends on the coordinating atomic species, their coordination number, and their Debye−Waller factors. Thus, by analyzing XAFS oscillations, one can derive information on the local environment around the excited atom. We excited the Pt L_3 edge (11.564 keV) to determine the local structure around the Pt atoms in the cluster.

We utilized the conventional method of XAFS analysis by extracting the oscillations from the spectrum by a background subtraction and then Fourier transforming the oscillations into real space. Various physically reasonable models were then constructed for the neighbors around the absorbing atom using the FEFF 6.01 program.[22] The FEFFIT program[23] was used to refine the fitting parameters of each model in r space. Because Pt and Ag are widely separated elements in the periodic table, they have a distinguishable backscattering amplitude and phase. Hence, it is much easier to detect and distinguish them in the XAFS measurement. A Pt foil was first measured in transmission mode XAFS for reference. In the Pt−Ag sample, XAFS measurements were performed at the Pt L_3 edge. These measurements showed that the Ag and Pt in these samples were not alloying. The first shell does not show any conspicuous trace of Ag; the central Pt is coordinated by only Pt atoms. The coordination number is much lower compared to that of bulk Pt, which is a reasonable characteristic of nanoparticle systems. More importantly, we observed a contraction in the Pt first shell bond length by 0.05 Å, as seen in Figure 2. This apparent reduction in bond length can be explained by the effect of

TABLE 2: List of Metal Compounds, Type of Capping Polymers, and Ag/Pt Mole Ratios Leading to, or Preventing, Nanowire Formation[a]

PVA molecular mass (amu), hydrolysis degree (%)	Ag/Pt mole ratio	Ag, Pt compounds	wire formation
31 000−170 000 and hydrolysis 87−89%	80/20 to 20/80	H_2PtCl_6 and Ag_2SO_4	yes
MW ≤ 20 000 or hydrolysis ≥ 98%	100/0 or 90/10 or 10/90 or 0/100	K_2PtCl_4 or $AgNO_3$	no

[a] All conditions in the second row must be met to produce nanowires; any condition met in the third row prevents nanowire formation. The aspect ratio of the nanoparticles did not depend on the total metal ion concentration (tested range: 1×10^{-4} to 2×10^{-3} mol/L) or the polymer concentration (tested range: 2 to 12 g/L) for solutions exposed to a total dose of 3.5 kGy.

disorder in XAFS,[22,24,25] which suggests that the Pt atoms in this sample are in a disordered state compared to those in the Pt foil. The formation of a homogeneous Ag−Pt alloy would lead to an expansion of the lattice parameter of Pt, as expected from Vegard's law and experimentally observed in ref 26. To corroborate our conclusion, we also performed an XAFS analysis of Ag−Pd nanoparticles produced with the radiolysis method.[27] The Pd bond length increased with increasing Ag mole ratio and indicated alloying of the two metals, in agreement with previous results from our group.[28] The XAFS analysis is also in agreement with the electrochemical arguments discussed earlier (eqs 5 and 6) and with previous experience with the radiolysis method. The less noble metal (Pt in our case) is reduced only after the more noble metal ions are exhausted, and it sticks to the preformed (Ag) seeds. In the resulting core−shell particles, the two metals are not alloyed and retain their bulk lattice parameter, as observed by XAFS.

The high aspect ratio of the nanoparticles produced in our experiments is apparently at odds with previous experiments, where radiolysis yielded nearly spherical Ag−Pt bimetallic clusters.[14] To better understand the nanowire formation mechanism, we varied numerous other parameters such as the total and relative metal and polymer concentrations, counterions, and type and molecular mass of the polymer. The effects of these parameters on the aspect ratio of the nanoparticles are summarized in Table 2. The most relevant parameters were the counterions, the mole ratio between the two metals, and the type of polymer employed. For example, when K_2PtCl_4 was employed, as in ref 14, spherical particles resulted. Similarly, nanowires did not form when $AgNO_3$ was employed instead of Ag_2SO_4. Nanowires also did not form when the Ag mole ratio was lower than 20% or higher than 80% of the total metal ion concentration. As for the polymer, we noticed that the degree of hydrolysis of the capping polymer, PVA, played an extremely important role. When PVA hydrolysis was on the order of 98−99%, spherical aggregates resulted. High aspect ratio nanoparticles were produced with 87−89% hydrolyzed PVA with a molecular weight of at least 31 000.

On the basis of the systematic variation of the experimental parameters, we will now illustrate what we think to be a possible scenario of nanowire formation. We will also show that the findings of our experiments are in good agreement with the general trends of the wet chemical synthesis of nanowires.[4−6,8,11] In most cases, nanowires are synthesized by reducing metal ions at a low rate in a micellar environment and out of metal cluster seeds. Although several details of the nanowire formation mechanism remain to be clarified, the interplay of these three parameters is qualitatively understandable. The seeds act as nucleation centers. The micelles, which can be cylindrical, provide a high aspect ratio template. Low reduction rates inhibit the formation of additional nuclei and force growth to be at the preformed seeds. In our case, the seeds are probably the Ag clusters that form in the initial stages of reduction, and the reduction rate is low because the radiation dose rate is low. We also have some evidence that polymer−metal complexes (and possibly micelles) are being formed. Partially hydrolyzed PVA can be envisaged as a copolymer, where hydrophilic vinyl alcohol groups are broken up by less hydrophilic, unhydrolyzed vinyl acetate groups. The unhydrolyzed groups are likely to aggregate in aqueous solution, presumably around hydrophilic species such as metal clusters or metal ions, possibly like a swollen micelle. The sensitivity of the synthesis to the presence of SO_4^{2-} and $PtCl_6^{2-}$ ions also suggests polymer−ion complex formation. For example, polymer gels of modified PVA show great sensitivity to the presence of ions such as sulfate.[29] These specific interactions probably enhance the interaction of the metal ions (and ultimately particles) with PVA. The polymer−metal complexes might be micelles since there is experimental evidence that copolymers made of hydrophilic and hydrophobic blocks, coordinated with metal ions, can give rise to micelles. For example, Ag nanowires have been obtained by reducing Ag^+ in the presence of block copolymers such as poly(ethylene oxide)−block−poly(methacrylic acid).[6] In these polymers, one block, poly(methacrylic acid), interacts strongly with Ag^+ ions whereas the other block interacts weakly. The strongly interacting block, when coordinated with Ag^+ ions, can become hydrophobic and form micelles.[30] Metal clusters formed within these micelles eventually aggregate to form nanowires.[6] We are planning additional experiments to clarify the nature and structure of the polymer−metal complexes and to clarify whether other parameters not considered in the present paper, such as intermolecular cross linking induced by gamma irradiation on PVA,[31] can affect nanowire formation.

In conclusion, we report a technique to synthesize high aspect ratio bimetallic nanostructures. We employed radiolysis to reduce metal ions in aqueous solution and generate filamentlike nanostructures that can be as long as several micrometers, with a diameter of a few nanometers. The filaments are polycrystalline and are made up of grains with fcc structure. The grains have probably a Ag core−Pt shell structure, homogeneous alloying being ruled out by XAFS. Key parameters for nanowire formation are the mole ratio between the two metals, the counterions, and the degree of hydrolysis of the PVA capping polymer. Additional experiments are planned to characterize the metal−polymer complexes and to extend our synthesis method to produce nanowires where the metals form homogeneous alloys.

Acknowledgment. We thank William Bonzer for his assistance in irradiating our samples. We also thank Dr. S. Miller for his assistance with TEM measurements. A.T.T., Director of the University of Missouri−Rolla Reactor (UMRR) Facility, thanks the Department of Energy for continued support of UMRR through the Reactor Instrumentation and Reactor Sharing Grant programs. The MRCAT beamline is supported by the U.S. DOE under grant number DEFG0200ER45811.

References and Notes

(1) Nicewarner-Pena, S. R.; Freeman, R. G.; Reiss, B. D.; He, L.; Pena, D. J.; Walton, I. D.; Cromer, R.; Keating, C. D.; Natan, M. J. *Science (Washington, D.C.)* **2001**, *294*, 137.

(2) Fukuoka, A.; Higashimoto, N.; Sakamoto, Y., Inagaki, S.; Fukushima, Y.; Ichikawa, M. *Top. Catal.* **2002**, *18*, 73.

(3) Filankembo, A.; Pileni, M. P. *J. Phys. Chem. B* **2000**, *104*, 5866.

(4) Pileni, M. P. *J. Phys. Chem*. **1993**, *97*, 6961.
(5) Pileni, M. P. *Langmuir* **1997**, *13*, 3266.
(6) Zhang, D.; Qi, L.; Ma, J.; Cheng, H. *Chem. Mater*. **2001**, *13*, 2753.
(7) Jana, N. R.; Gearheart, L.; Murphy, C. J. *Chem. Mater*. **2001**, *13*, 2313.
(8) Murphy, C. J.; Jana, N. R. *Adv. Mater*. **2002**, *14*, 80.
(9) Jana, N. R.; Gearheart, L.; Murphy, C. J. *J. Phys. Chem. B* **2001**, *105*, 4065.
(10) Jana, N. R.; Gearheart, L.; Murphy, C. J. *Chem. Commun.* **2001**, 617.
(11) Sun, Y.; Gates, B.; Mayers, B.; Xia, Y. *Nano Lett.* **2002**, *2*, 165.
(12) Zhou, Y.; Yu, S. H.; Wang, C. Y.; Li, X. G.; Zhu, Y. R.; Chen, Z. Y. *Adv. Mater*. **1999**, *11*, 850.
(13) Belloni, J.; Mostafavi, M.; Remita, H.; Marignier, J. L.; Delcourt, M. O. *New J. Chem*. **1998**, 1239.
(14) Treguer, M.; de Cointet, C.; Remita, S.; Khatouri, M.; Mostafavi, M.; Amblard, J.; Belloni, J. *J. Phys. Chem. B* **1998**, *102*, 4310.
(15) Marignier, J. L.; Belloni, J.; Delcourt, M. O.; Chevalier, J. P. *Nature (London)* **1985**, *317*, 344.
(16) Remita, H.; Mostafavi, M.; Delcourt, M. O. *Radiat. Phys. Chem.* **1996**, *47*, 275.
(17) Henglein, A. *Isr. J. Chem.* **1993**, *33*, 77.
(18) For some mole ratios and irradiation doses, the metal ions in the solutions were not completely reduced. For example, the spectra of Figure 1e show an absorption band at about 250 nm, characteristic of solvated Pt complexes. Nanowire formation was found to be independent of the reduction degree of the metal ions.
(19) Liz-Marzan, L. M.; Philipse, A. P. *J. Phys. Chem.* **1995**, *99*, 15120.
(20) Kreibig, U.; Gartz, M.; Hilger, A. *Ber. Bunsen-Ges. Phys. Chem.* **1997**, *101*, 1593.
(21) *X-ray Absorption: Principles, Applications, Techniques of EXAFS, SEXAFS and XANES;* Koningsberger, D. C., Prins, R., Eds.; Wiley & Sons: New York, 1988
(22) Newville, M.; Ravel, B.; Haskel, D.; Rehr, J. J.; Stern, E. A.; Yacobi, Y. *Physica B* **1995**, *208*−*209*, 154.
(23) Newville, M. *J. Synth. Radiat*. **2001**, *8*, 96.
(24) Dalba, G.; Fornasini, P.; Grisenti, R.; Pasqualini, D.; Diop, D.; Monti, F. *Phys. Rev. B* **1998**, *58*, 4793.
(25) Rossner, H.; Krappe, H. *J. Synth. Radiat*. **2001**, *8*, 261.
(26) Torigoe, K.; Nakajima, Y.; Esumi, K. *J. Phys. Chem.* **1993**, *97*, 8304.
(27) Doudna, C. M.; Bertino, M. F.; Tokuhiro, A. T.; Terry, J.; Blum, F. D., to be submitted for publication.
(28) Doudna, C. M.; Bertino, M. F.; Tokuhiro, A. T. *Langmuir* **2002**, *18*, 2434.
(29) Okazaki, Y.; Ishizuki, K.; Kawauchi, S.; Satoh, M.; Komiyama, J. *Macromolecules* **1996**, *29*, 8391.
(30) Colfen, H. *Macromol. Rapid Commun.* **2001**, *22*, 219.
(31) Wang B.; Mukataka S.; Kodama M.; Kokufuta E. *Langmuir* **1997**, *13*, 6108.